EFFECTS OF NOTCHES ON ELEVATED-TEMPERATURE, LOW-CYCLE FATIGUE BEHAVIOR OF TYPE 204 STAINLESS STEEL

by

D. T. Raske and P. S. Maiya

Prepared for

Symposium on

Ductility and Toughness Considerations in Elevated Temperature Service

1978 ASME Winter Annual Meeting

San Francisco, California

December 10-15, 1978

U of C-AUA-USDOE

ARGONNE NATIONAL LABORATORY, ARGONNE, ILLINOIS

Operated under Contract W-31-109-Eng-38 for the

U. S. DEPARTMENT OF ENERGY

Effects of Notches on Elevated-temperature, Low-cycle Fatigue Behavior of Type 304 Stainless Steel*

by

D. T. Raske and P. S. Maiya

Materials Science Division
ARGONNE NATIONAL LABORATORY
Argonne, Illinois 60439

Abstract

The results of an investigation into the effects of geometric stress concentrations on the elevated-temperature low-cycle fatigue behavior of Type 304 stainless steel are presented. The principal objective of this study was to develop a data base that could be used to verify the ASME Code Case 1592-8 design method for predicting the creep-fatigue behavior of structural components which contain discontinuities. In continuous-cycling tests, the local strains at the notch root determined from the Code Case procedure result in fatigue-life estimates that are conservative when compared to the experimental values. For tests containing a hold time at the peak tensile strain, the Code Case procedure results in local strains that are nearly identical to the experimentally obtained local strains, if the local stress is assumed to relax to the nominal value during the hold time.

---

*Work supported by the U.S. Department of Energy.

Effects of Notches on Elevated-temperature, Low-cycle Fatigue Behavior of Type 304 Stainless Steel*

by

D. T. Raske and P. S. Maiya

Materials Science Division
ARGONNE NATIONAL LABORATORY
Argonne, Illinois 60439

Introduction

Type 304 stainless steel will be one of the primary materials used in the fabrication of liquid metal fast breeder reactor vessels and components. Since these systems operate at elevated temperatures and are subject to a variety of cyclic and static loading conditions, a number of studies have been performed on the creep-fatigue behavior of this material using unnotched specimens [1].** The present paper describes the results of an investigation into the effects of geometric stress concentrations on the elevated-temperature low-cycle fatigue behavior of Type 304 stainless steel.

Although methods for calculating strains due to geometric discontinuities under cyclic loadings are specified in the ASME code case [2], no investigation has been undertaken to verify these design rules. Thus, the principal objective of the present study was to develop a sufficient date base for the verification of a design method to predict the creep-fatigue behavior of structural components which contain discontinuities.

The present paper contains the results of fatigue tests at 593°C in air using circumferentially notched specimens with theoretical elastic stress-

---

*Work supported by the U.S. Department of Energy.

**Numbers in brackets designate References at end of paper.

concentration factors, K_t, of 1.5, 2.0, 3.0, and 4.0. Continuous-cycling tests, as well as tests with a hold time at the peak tensile strain, are included. The effect of the notch-root, or local, strain rate was also investigated by tests with $\dot{\varepsilon} \sim 4 \times 10^{-3}$ and $4 \times 10^{-5}\ s^{-1}$. In addition, the results of several tests at 482°C are reported. The fatigue lives obtained from these tests are compared with those predicted by means of the procedure outlined in ASME Code Case 1592-8 [2].

Experimental

The chemical composition of the Type 304 stainless steel used (Heat 9T2976) is provided in Ref. 3. Prior to testing, the specimens were solution annealed in evacuated quartz tubes back-filled with argon for 1800 s at 1092°C, and then aged at 593°C for 3.6×10^6 s.

Axially loaded specimens with circumferential notches were employed (Fig. 1). The notch geometry was such that the theoretical elastic stress-concentration factors, K_t, were 1.5, 2.0, 3.0, and 4.0 [4]. To minimize residual stresses, the notches were machined with successively lighter tool cuts. The final 0.025 mm of material at the notch root was removed by mechanical polishing. The resultant finish at the notch root had a ~0.025-μm surface roughness. A 50X optical comparator was used to determine the final notch dimensions.

Tests were conducted in a closed-loop hydraulic system that was operated in the load-control mode. The specimens were subjected to fully reversed axial loadings, using a triangular waveform. Specimen heating was accomplished by an induction coil that operated at 455 KHz. The coil was designed to provide a flat temperature profile over a distance of ~6 mm on either side of the notch. With this coil arrangement, the temperature at the notch root was within 5°C of the controlled surface temperature.

Groups of specimens with constant values of K_t were tested in the life range of $\sim 10^2$-10^5 cycles. Cyclic frequencies that correspond to calculated notch-root-material strain rates of $\sim 4 \times 10^{-3}$ and $\sim 4 \times 10^{-5}$ s^{-1} were employed. Neuber's rule [5] was used to estimate these frequencies prior to testing. This rule is expressed by the equation

$$K_t = (K_\sigma K_\varepsilon)^{1/2} , \tag{1}$$

where K_σ is the stress-concentration factor (the stress range at the notch root, $\Delta\sigma$, divided by the nominal stress range over the net area, Δs) and K_ε is the strain-concentration factor (the strain range at the notch root, $\Delta\varepsilon$, divided by the nominal strain range over the net area, Δe). The cyclic stress-strain curves used in conjunction with Neuber's rule was obtained from continuous-cycling fatigue data on material from the same heat and with the same heat treatment as in the present study. Values of the notch-root stress and strain were obtained by the usual assumption that both smooth and notched samples will have equal fatigue lives if the same stress and strain ranges are present at the location of crack initiation. This procedure is shown schematically in Fig. 2. Another assumption was that, after initial readjustments, the material at the notch root is subject to conditions approximating reversed strain cycling [6].

Results

The results for the continuous-cycling and tension hold-time tests are listed in Tables 1 and 2. Included are the controlled nominal stress ranges, fatigue lives, cyclic frequencies, and the nominal strain ranges determined from the nominal stress ranges using the cyclic stress-strain curves. The local stress and strain ranges were determined from the unnotched specimen strain-life curves and the cyclic stress-strain curves previously described. Average local strain rates were calculated from the cyclic frequencies and the local strain ranges. Comparisons of the notched specimen data with unnotched specimen data are shown in Figs. 3, 4 and 5. The curves for the unnotched specimens were obtained by a multivariable regression analysis of data from tests between 430 and 816°C [1]. The curves for the notched specimens are plotted in terms of the nominal strain range, Δe. Arrows on three data points in Figs. 3 and 4 indicate specimens that did not fail. In general, presence of notches reduces fatigue life principally by expediting the crack-initiation process. As in the case of smooth specimens, fatigue life decreases with a decrease in the (calculated) notch-root strain rates. For example, the notch-fatigue life can decrease approximately by a factor of two with a decrease in strain rate from $4 \times 10^{-3}\ s^{-1}$ to $4 \times 10^{-5}\ s^{-1}$.

The continuous-cycling notched-specimen nominal strain amplitudes, e, were also used to obtain fatigue lives predicted by the ASME Code Case procedure [2]. This procedure results in a total equivalent strain amplitude given by

$$\varepsilon = \frac{S^*}{\bar{S}} K_t^2 e , \tag{2}$$

where S^* and $\bar{S}$ are defined in Fig. 6. Values of ε calculated by Eq. (2) were then used with the unnotched specimen strain-life curves of Figs. 3-5 to predict the fatigue lives of the notched specimens. Tables 3 and 4 list the values of the terms in Eq. (2), the predicted fatigue lives, and the experimentally observed fatigue lives from these tests. A comparison of the experimentally observed and predicted fatigue lives for these data and the data reported previously is shown in Fig. 7. It is apparent from this figure that Eq. (2) generally underpredicts the experimentally observed life, especially for the specimens with higher values of K_t.

In creep-fatigue tests, Eq. (2) is modified to account for the creep strain accumulated during the hold time [2]. This results in a relation in which the total equivalent strain is given by

$$\varepsilon = \frac{S^*}{\overline{S}} K_t^2 e + K_t e_c \ , \quad (3)$$

where e_c is the creep strain. In addition, the cyclic stress-strain curve is modified by shifting the origin downward along the elastic line by an amount equal to the stress relaxation, S_r, during the hold period, as shown in Fig. 8. Values for the creep strain were obtained from the product of the cyclic plastic creep rate, $\dot{\varepsilon}_p$, and the hold time. The cyclic plastic creep rate for Type 304 stainless steel at 593°C was determined from creep-fatigue data on unnotched specimens and is given by [7]

$$\dot{\varepsilon}_p = 2.503 \times 10^{-11} (\sigma)^{1.681} \ s^{-1} \ , \quad (4)$$

where σ is the applied stress. For this analysis it is assumed that, for notched specimens under tensile hold-time conditions, the maximum local stress relaxes to some lower value, S_r, almost immediately after the beginning of the hold-time period. Thus, the applied stress in Eq. (4) equals the relaxed stress. In these tests, the nominal stress amplitude of 143.4 MPa and nominal strain amplitude of 0.18% result in a maximum local stress of $\overline{S}$ = 208.4 MPa before relaxation occurs.

When Eq. (3) is used to calculate notch-root strains under hold-time conditions, a definition of relaxed stress (S_r in Fig. 8) is required. For the present purpose, it was assumed that the local stress relaxes to different levels of stress (between local stress and nominal stress), and the notch-root strain was calculated for varying amounts of stress relaxation. The results obtained are listed in Table 5 and shown in Fig. 9. It is found that agreement between the observed and predicted lives is obtained only when the local stress is assumed to relax rapidly to the nominal stress (100% stress relaxation) followed by cyclic creep during tensile hold time. For the cases in which stress relaxation of <100% is assumed, the predicted life underpredicts the experimental fatigue life. An additional indication of the validity of this observation is obtained when the calculated local strains at 100% stress relaxation in Table 5 are compared with the experimentally determined local strains in Table 1.

Conclusions

The results of elevated-temperature continuous-cycling and tension hold-time load-control tests on circumferentially notched specimens of Type 304 stainless steel lead to the following conclusions:

(a) In the case of continuous-cycling tests, the ASME Code Case 1592-8 procedure for determining the equivalent local strain at the notch root results in fatigue-life estimates that are conservative when compared with actual experimental values. Moreover, the life estimates become increasingly more conservative as the theoretical elastic-stress-concentration factor increases.

(b) For tests containing a hold time, the Code Case procedure results in equivalent local strains that are nearly identical to the local strains obtained by a comparison of the notched-specimen fatigue lives with unnotched-specimen lives, if the local stress is assumed to relax to the nominal stress during the hold time. For lesser amounts of local stress relaxation, the Code Case procedure results in conservative estimates of notched-specimen fatigue lives.

References

1. Diercks, D. R. and Raske, D. T., *Elevated-temperature, Strain-controlled Fatigue Data on Type 304 Stainless Steel -- A Compilation, Multiple Linear Regression Model, and Statistical Analysis*, Argonne National Laboratory, ANL-76-95 (1976).

2. *ASME Boiler and Pressure Vessel Code, Case 1592-8*, American Society of Mechanical Engineers, New York, 1976, p. 392.

3. Cheng, C. Y. and Diercks, D. R., "Effects of Hold Time on Low-cycle Fatigue Behavior of AISI Type 304 Stainless Steel at 593°C," *Met. Trans.* 4:615-617 (1973).

4. Peterson, R. E., *Stress Concentration Design Factors*, John Wiley and Sons, New York, 1953.

5. Neuber, H., "Theory of Stress Concentration for Shear Strained Prismatical Bodies with Aribtrary Non Linear Stress Strain Law," *Appl. Mech.* 28:544-550 (1961).

6. Dolan, T. J., "Non-Linear Response Under Cyclic Loading Conditions," *Proceedings of the Ninth Midwest Mechanics Conference*, August 1965, pp. 3-21.

7. Majumdar, S. and Maiya, P. S., *A Unified and Mechanistic Approach to Creep-Fatigue Damage*, Argonne National Laboratory, ANL-76-58 (1976).

Table 1. Summary of Results of Notched Type 304 Stainless Steel Specimens at 482 and 593°C with $\dot{\varepsilon} \approx 4 \times 10^{-3}\ s^{-1}$

Specimen Number	K_t	Nominal Stress Range ΔS, MPa	Tensile Hold Time, s	Cycles to Failure, N_f	Cyclic Frequency, H_z	Nominal Strain Range Δe, %	Local Strain Range Δε, %	Local Strain Rate, $\dot{\varepsilon} \times 10^{-3}\ s^{-1}$	Local Stress Range Δσ, MPa	Kσ Stress Concentration, Δσ/ΔS	K_ε Strain Concentration, Δε/Δe
						482°C					
N-27	2.0	394.1	0	4160	0.133	0.67	1.14	3.0	524.0	1.33	1.70
N-35	2.0	336.5	0	5576	0.211	0.50	1.02	4.3	493.7	1.46	1.92
N-42	2.0	262.0	0	25357	0.400	0.33	0.62	5.0	383.3	1.46	1.82
N-40	2.0	220.6	0	>410228[a]	0.400	0.25	-	-	-	-	-
						593°C					
N-14	1.5	526.1	0	1180	0.100	1.17	1.60	3.2	608.1	1.16	1.37
N-15	1.5	459.2	0	1456	0.133	0.88	1.44	3.8	579.2	1.26	1.64
N-13	1.5	309.6	0	6324	0.268	0.42	0.76	4.1	426.1	1.33	1.81
N-12	1.5	255.8	0	>406000[a]	0.400	0.30	-	-	-	-	-
N-11	2.0	553.6	0	228[b]	0.080	1.30	4.00	6.4	~913	~1.65	3.08
N-8	2.0	437.1	0	1205	0.100	0.80	1.60	3.2	608.1	1.39	2.00
N-7	2.0	361.3	0	2685	0.200	0.55	1.09	4.4	508.8	1.41	1.98
N-10	2.0	311.6	0	4725	0.267	0.42	0.85	4.5	450.9	1.45	2.02
N-9	2.0	277.8	0	15752	0.400	0.34	0.55	4.4	359.9	1.29	1.62
N-45	2.0	286.8	600	2174	0.200	0.36	0.62	2.5	382.0	1.33	1.72
N-44	2.0	286.8	3600	794	0.200	0.36	0.70	2.8	408.2	1.42	1.94
N-41	2.0	286.8	10800	425	0.200	0.36	0.83	3.3	445.4	1.55	2.30
N-5	3.0	446.1	0	397[b]	0.100	0.83	2.90	5.8	~806	~1.81	3.49
N-2	3.0	357.8	0	2126	0.200	0.55	1.20	4.8	532.3	1.49	2.18
N-23	3.0	299.9	0	3487	0.233	0.39	0.96	4.5	479.9	1.60	2.46
N-1	3.0	248.2	0	9708	0.400	0.28	0.65	5.2	393.0	1.58	2.32
N-6	3.0	232.4	0	48216	0.400	0.25	0.41	3.3	306.1	1.32	1.64
N-4	3.0	197.2	0	>553000[a]	0.400	0.20	-	-	-	-	-
N-18	4.0	406.1	0	744	0.100	0.69	2.04	4.1	675.7	1.66	2.96
N-17	4.0	345.4	0	1635	0.100	0.51	1.37	2.7	566.7	1.64	2.68
N-19	4.0	271.6	0	3789	0.100	0.32	0.93	1.9	471.6	1.74	2.91
N-20	4.0	208.2	0	21271	0.400	0.21	0.50	4.0	342.0	1.64	2.38

[a] Specimen did not fail.

[b] Specimen may have buckled prior to failure.

Table 2. Summary of Results for Notched Type 304 Stainless Steel Specimens at 593°C with $\dot{\varepsilon} \approx 4 \times 10^{-5}$ s^{-1}

Specimen Number	K_t	Nominal Stress Range ΔS, MPa	Cycles to Failure, N_f	Cyclic Frequency, H_z	Nominal Strain Range Δe, %	Local Strain Range $\Delta\varepsilon$, %	Local Strain Rate, $\dot{\varepsilon} \times 10^{-5}$ s^{-1}	Local Stress Range $\Delta\sigma$, MPa	K_σ Stress Concentration, $\Delta\sigma/\Delta s$	K_ε Strain Concentration, $\Delta\varepsilon/\Delta e$
N-39	2.0	424.7	524	0.00133	0.76	1.63	4.4	613.6	1.44	2.14
N-33	2.0	341.3	1,497	0.00200	0.50	0.96	3.8	479.9	1.41	1.92
N-38	2.0	291.7	5,299	0.00267	0.37	0.59	3.2	372.3	1.28	1.59
N-37	2.0	273.0	12,935	0.00400	0.33	0.45	3.6	322.7	1.18	1.36
N-28	4.0	369.6	533	0.00133	0.58	1.63	4.4	613.6	1.66	2.81
N-32	4.0	311.6	1,027	0.00200	0.42	1.16	4.6	524.0	1.68	2.76
N-26	4.0	282.7	2,696	0.00200	0.35	0.75	3.0	423.3	1.47	2.14
N-30	4.0	253.7	4,586	0.00400	0.29	0.62	5.0	383.3	1.51	2.14
N-29	4.0	231.7	7,046	0.00400	0.25	0.54	4.3	355.8	1.54	2.16

Table 3. Comparison of Predicted and Experimentally Observed Fatigue Lives for Notched Specimens of Type 304 Stainless Steel at 482 and 593°C with $\dot{\varepsilon} \approx 4 \times 10^{-3}\ s^{-1}$

Specimen Number	K_t	e, %	$K_t e$, %	S*, MPa	$\overline{S}$, MPa	ε, %	N_f, Cycles (Predicted)	N_f, Cycles (Experimental)
				482°C				
N-27	2.0	0.34	0.68	197.0	284.6	0.93	1361	4160
N-35	2.0	0.25	0.50	168.2	245.8	0.69	2639	5576
N-42	2.0	0.17	0.34	131.0	195.4	0.44	8438	25357
				593°C				
N-14	1.5	0.59	0.89	262.9	319.8	1.08	662	1180
N-15	1.5	0.44	0.66	229.3	278.4	0.82	1137	1456
N-13	1.5	0.21	0.32	156.0	194.8	0.38	6372	6324
N-11	2.0	0.65	1.30	275.8	379.2	1.89	244	228
N-8	2.0	0.40	0.80	217.2	305.0	1.14	599	1205
N-7	2.0	0.28	0.55	181.9	255.1	0.78	1225	2685
N-10	2.0	0.21	0.42	156.0	224.1	0.59	2263	4725
N-9	2.0	0.17	0.34	137.9	202.6	0.46	3867	15752
N-5	3.0	0.42	1.26	222.4	372.3	2.23	184	397
N-2	3.0	0.28	0.87	181.0	309.4	1.45	387	2126
N-23	3.0	0.20	0.59	150.0	263.6	1.00	3225	3487
N-1	3.0	0.14	0.42	123.3	224.1	0.69	1569	9708
N-6	3.0	0.13	0.39	114.7	212.0	0.61	2066	48216
N-18	4.0	0.35	1.40	203.4	388.7	2.89	120	744
N-17	4.0	0.26	1.04	174.1	337.8	2.10	204	1635
N-19	4.0	0.16	0.64	133.6	274.1	1.25	506	3789
N-20	4.0	0.11	0.44	103.4	224.1	0.78	1257	21271

Table 4. Comparison of Predicted and Experimentally Observed Fatigue Lives for Notched Specimens of Type 304 Stainless Steel at 593°C and $\dot{\varepsilon} \approx 4 \times 10^{-5}\ s^{-1}$

Specimen Number	K_t	e, %	$K_t e$, %	S*, MPa	$\overline{S}$, MPa	ε, %	N_f, Cycles (Predicted)	N_f, Cycles (Experimental)
N-39	2.0	0.38	0.76	212.4	297.4	1.09	329	524
N-33	2.0	0.25	0.50	170.7	243.4	0.70	707	1497
N-38	2.0	0.19	0.38	145.8	210.3	0.51	1299	5299
N-37	2.0	0.17	0.34	136.5	199.6	0.45	1734	12935
N-28	4.0	0.29	1.16	184.8	361.3	2.37	100	533
N-32	4.0	0.21	0.84	155.8	312.3	1.68	165	1027
N-26	4.0	0.18	0.72	141.3	285.8	1.39	222	2696
N-30	4.0	0.15	0.60	126.9	261.2	1.13	310	4586
N-29	4.0	0.13	0.52	115.8	243.4	0.95	411	7046

Table 5. Comparison of Predicted[a] and Experimentally Observed Tensile Hold-time Fatigue Life for Notched Specimens of Type 304 Stainless Steel at 593°C. $K_t = 2$, $S = 143.4$ MPa, $e = 0.18\%$, and $\dot{\varepsilon} \approx 4 \times 10^{-3}\ s^{-1}$

Specimen Number	Hold Time, s	Local Strain Range $\Delta\varepsilon$, % (Eq. 2)	N_f, Cycles (Predicted)	N_f, Cycles (Experimental)
		0% Stress Relaxation		
N-45	600	1.02	802	2174
N-44	3600	1.14	361	794
N-41	10800	1.43	201	425
		50% Stress Relaxation		
N-45	600	0.80	1280	2174
N-44	3600	0.88	533	794
N-41	10800	1.10	283	425
		100% Stress Relaxation[b]		
N-45	600	0.64	2028	2174
N-44	3600	0.70	790	794
N-41	10800	0.85	407	425

[a]Predicted life is based on guidelines given in the ASME Code Case.

[b]Maximum stress at the notch root relaxes to nominal stress.

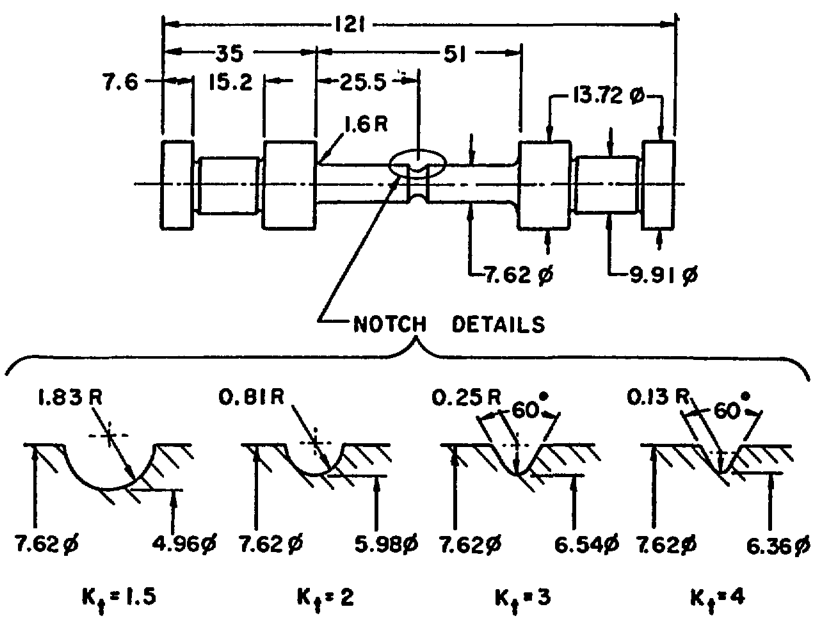

Fig. 1. Notched specimen details. Neg. No. MSD-63467.

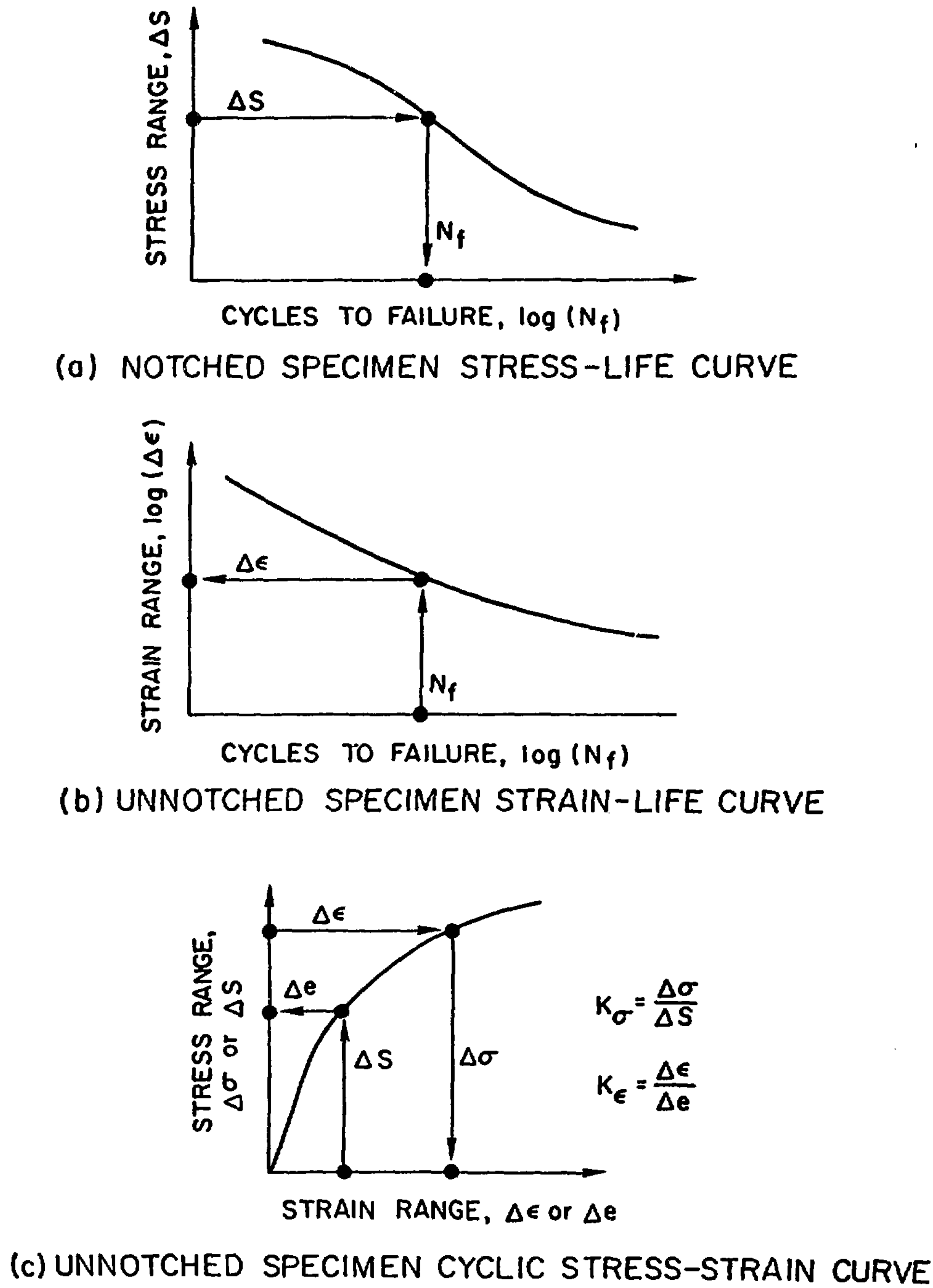

Fig. 2. Curves used to determine K values in Neuber's equation. Neg. No. MSD-63466.

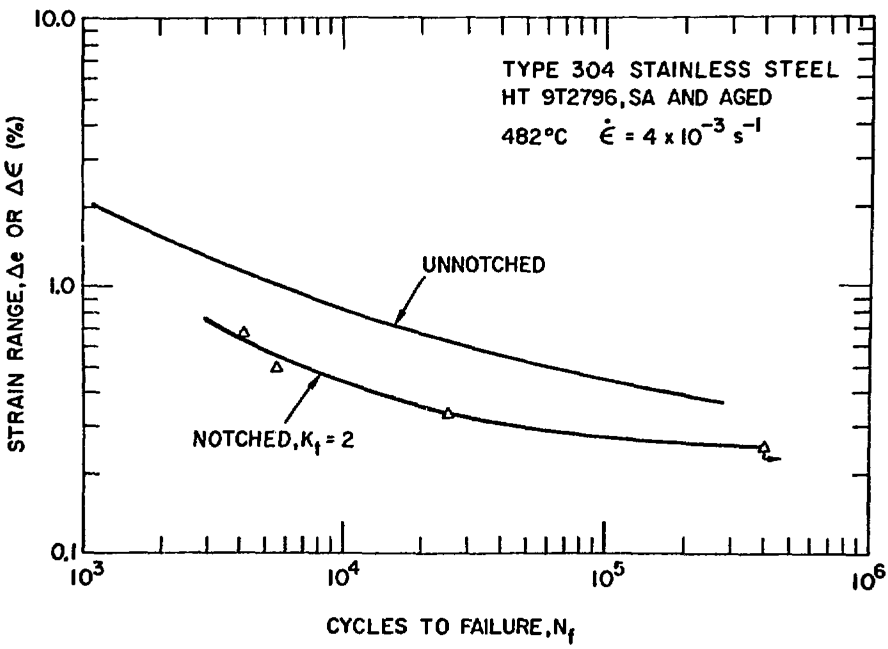

Fig. 3. Continuous-cycling Strain-life curves for Type 304 stainless steel at 482°C and $\dot{\varepsilon} = 4 \times 10^{-3}$ s^{-1}. Neg. No. MSD-64853.

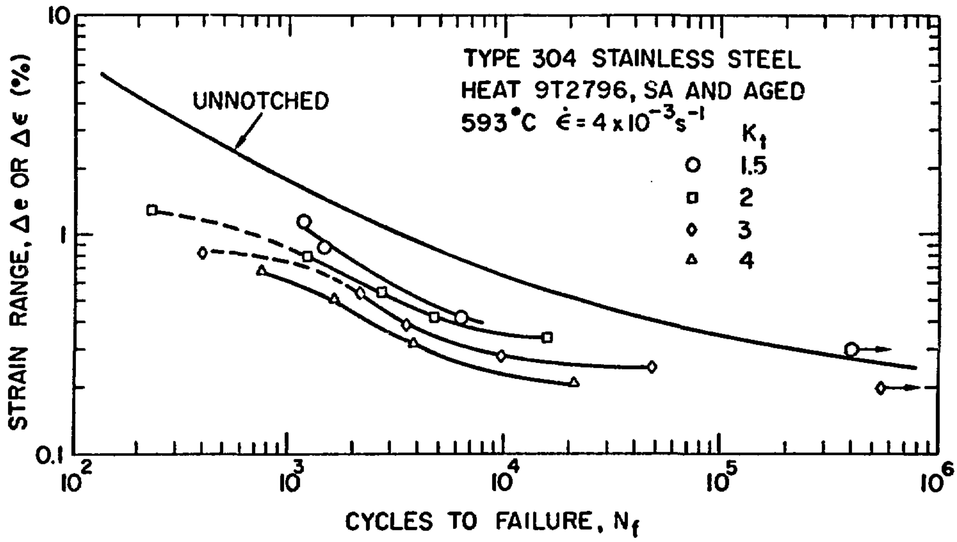

Fig. 4. Continuous-cycling strain-life curves for Type 304 stainless steel at 593°C and $\dot{\varepsilon} = 4 \times 10^{-3}\ s^{-1}$. Neg. No. MSD-65133.

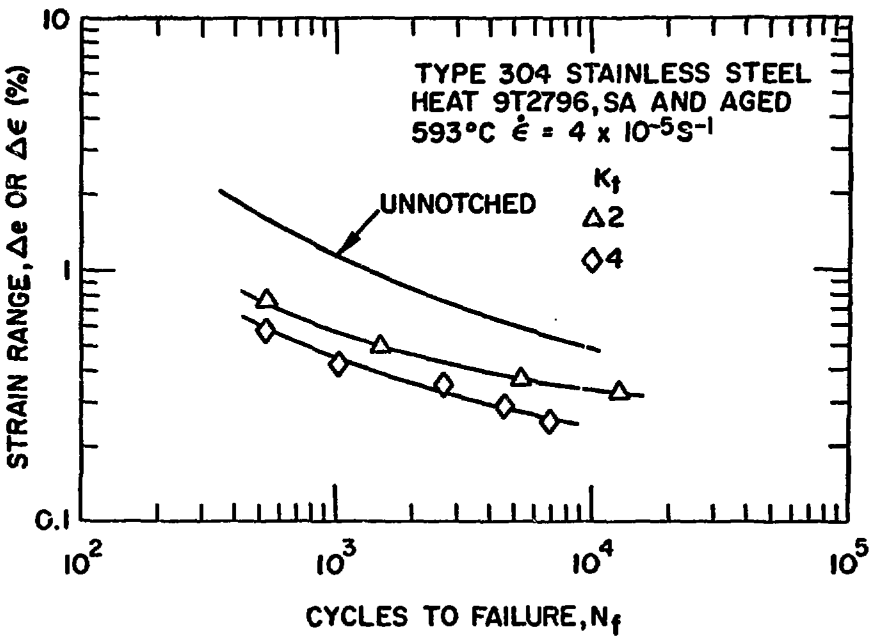

Fig. 5. Continuous-cycling strain-life curves for Type 304 stainless steel at 593°C and $\dot{\epsilon} = 4 \times 10^{-5}\ s^{-1}$. Neg. No. MSD-64044.

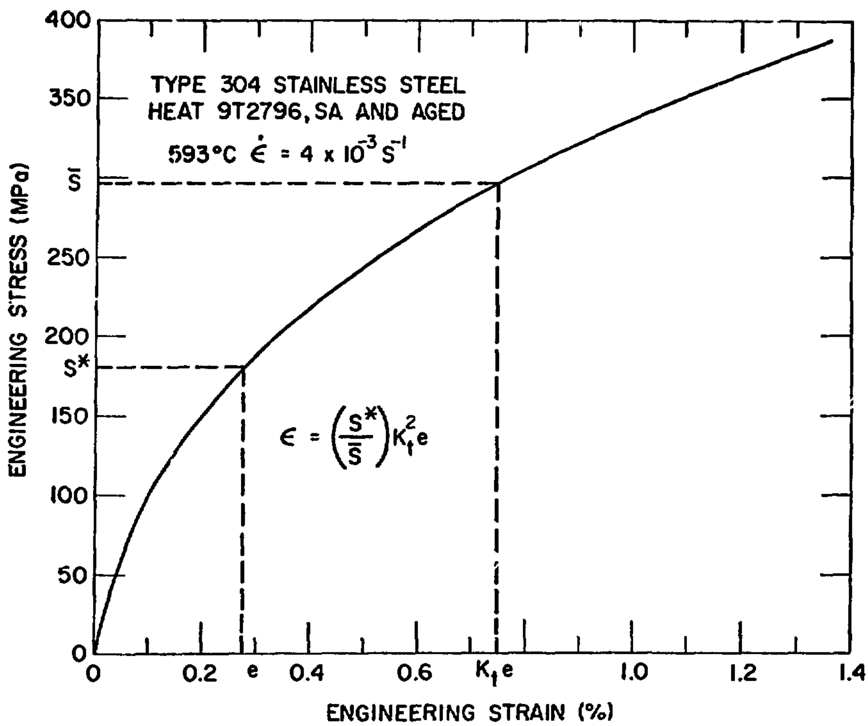

Fig. 6. Cyclic stress-strain curve showing the definition of S^* and $\bar{S}$. Neg. No. MSD-64045.

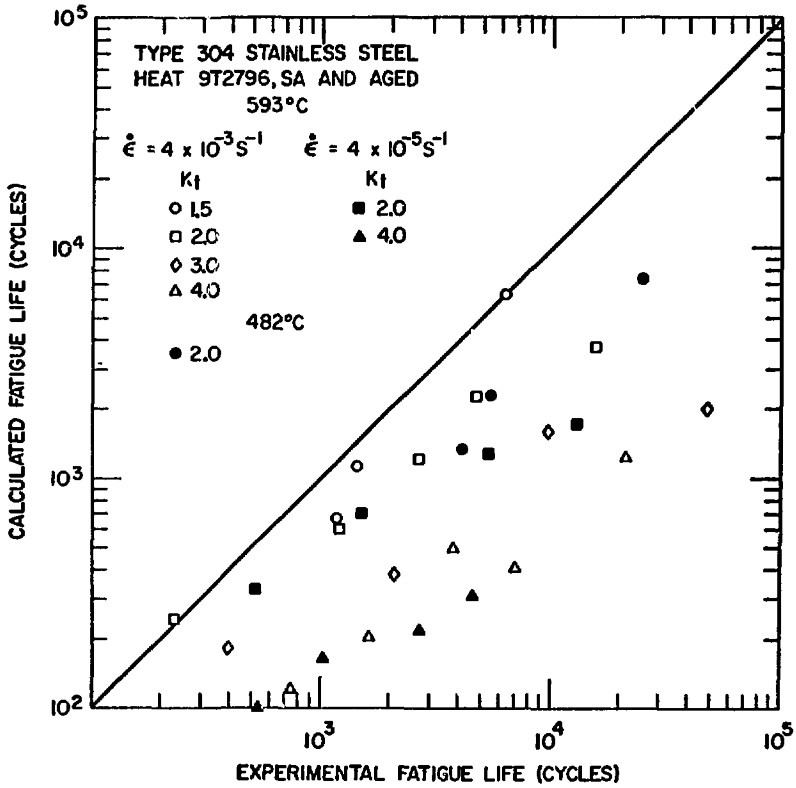

Fig. 7. Comparison of predicted fatigue life with experimental fatigue life for notched specimens of Type 304 stainless steel. Neg. No. ANL-306-77-228.

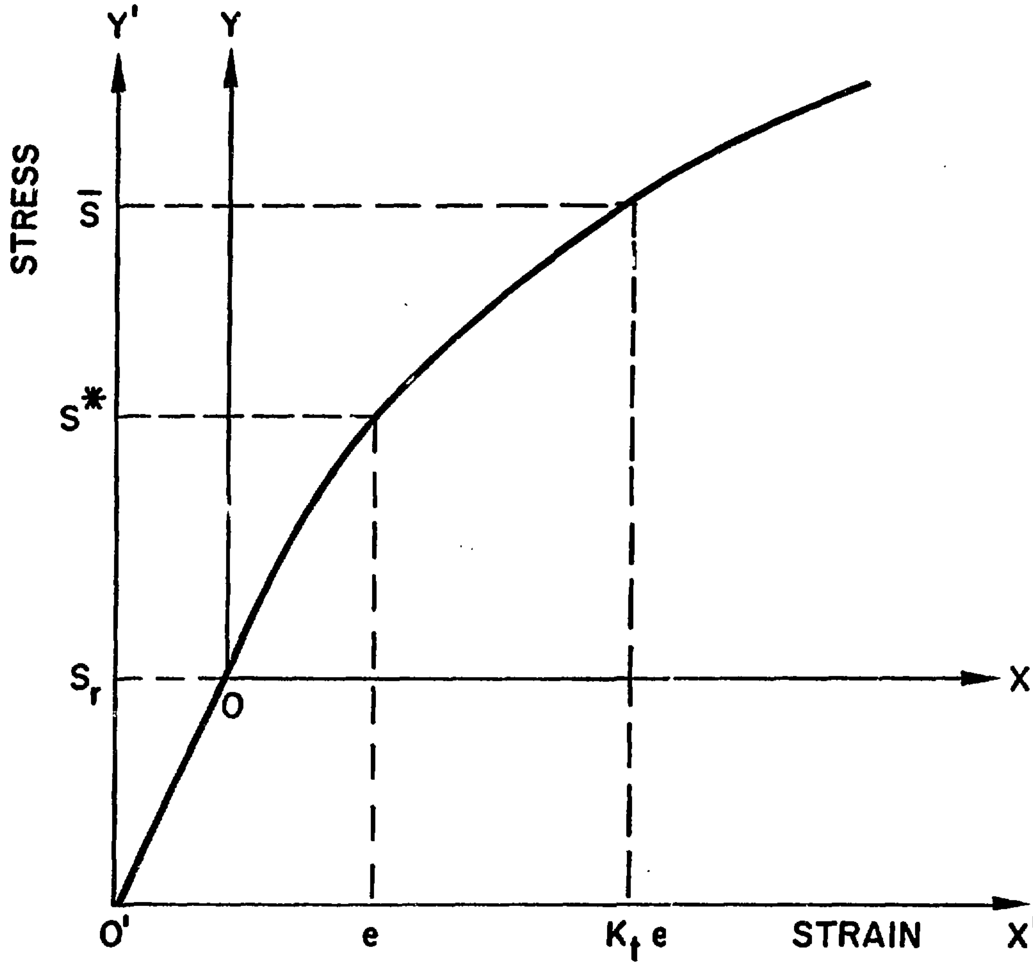

$$\epsilon = \left(\frac{S^*}{\bar{S}}\right) K_t^2 e + K_t e_c$$

Fig. 8. Cyclic stress-strain curve showing the definition of S* and $\overline{S}$ for hold-time notch fatigue tests. Neg. No. ANL-306-77-649.

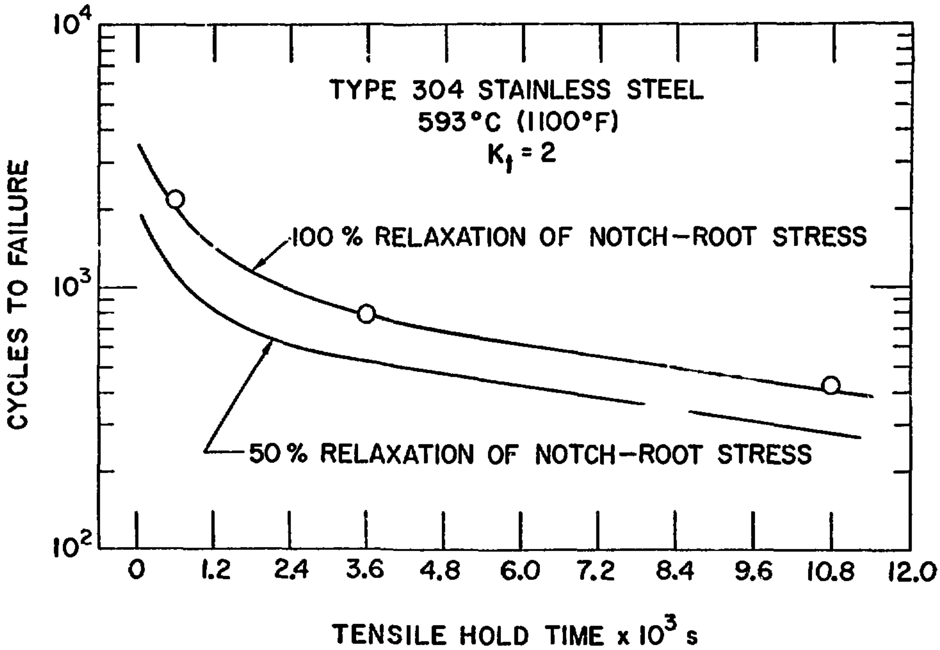

Fig. 9. Comparison of predicted experimental fatigue life. Symbols represent experimental results; curves represent predicted results. Neg. No. MSD-64854.